High-dimensional Motion Segmentation by Variational Autoencoder and Gaussian Processes

Masatoshi Nagano[1,*], Tomoaki Nakamura[1], Takayuki Nagai[2], Daichi Mochihashi[3], Ichiro Kobayashi[4] and Wataru Takano[2]

Abstract— **Humans perceive continuous high-dimensional information by dividing it into significant segments such as words and units of motion. We believe that such unsupervised segmentation is also important for robots to learn topics such as language and motion. To this end, we previously proposed a hierarchical Dirichlet process–Gaussian process–hidden semi-Markov model (HDP-GP-HSMM). However, an important drawback to this model is that it cannot divide high-dimensional time-series data. Further, low-dimensional features must be extracted in advance. Segmentation largely depends on the design of features, and it is difficult to design effective features, especially in the case of high-dimensional data. To overcome this problem, this paper proposes a hierarchical Dirichlet process–variational autoencoder–Gaussian process–hidden semi-Markov model (HVGH). The parameters of the proposed HVGH are estimated through a mutual learning loop of the variational autoencoder and our previously proposed HDP-GP-HSMM. Hence, HVGH can extract features from high-dimensional time-series data, while simultaneously dividing it into segments in an unsupervised manner. In an experiment, we used various motion-capture data to show that our proposed model estimates the correct number of classes and more accurate segments than baseline methods. Moreover, we show that the proposed method can learn latent space suitable for segmentation.**

I. Introduction

Humans perceive continuous high-dimensional information by dividing it into significant segments such as words and units of motion. For example, we recognize words by segmenting speech waves, and we perceive particular motions by segmenting continuous motion. Humans learn words and motions by appropriately segmenting continuous information without explicit segmentation points. We believe that such unsupervised segmentation is also important for robots, in order for them to learn language and motion.

To this end, we previously proposed a hierarchical Dirichlet process–Gaussian process–hidden semi-Markov model (HDP-GP-HSMM) [1]. HDP-GP-HSMM is a nonparametric Bayesian model that is a hidden semi-Markov model whose emission distributions are Gaussian processes, making it possible to segment time-series data in an unsupervised manner. In this model, segments are continuously represented using a Gaussian process. Moreover, the number of segmented classes can be estimated using hierarchical Dirichlet processes [2]. The Dirichlet processes assume an infinite number of classes. However, only a finite number of classes are actually used. This is accomplished by stochastically truncating the number of classes using a slice sampler [3].

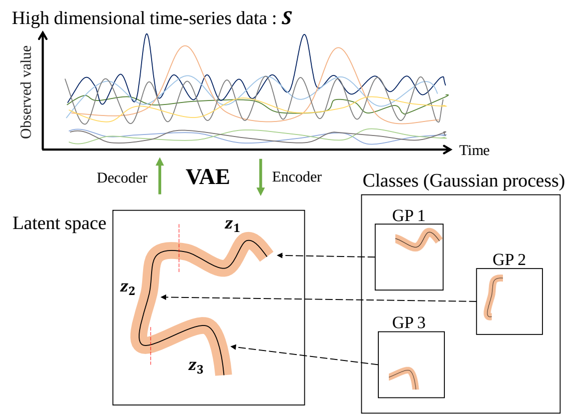

Fig. 1. Overview of the generative process of the HVGH.

However, our HDP-GP-HSMM cannot deal with high-dimensional data, and feature extraction is needed in order to reduce the dimensionality in advance. Indeed, segmentation largely depends on this feature extraction, and it is difficult to extract effective features, especially in the case of high-dimensional data. To overcome this problem, this paper introduces a variational autoencoder (VAE) [4] to the HDP-GP-HSMM. Thus, the model we propose in this paper is a hierarchical Dirichlet process–variational autoencoder–Gaussian process–hidden semi-Markov model (HVGH). Fig. 1 shows an overview of HVGH. The observation sequence is compressed and converted into a latent variable sequence by the VAE, and the latent variable sequence is divided into segments by HDP-GP-HSMM. Furthermore, parameters learned by HDP-GP-HSMM are used as the hyperparameters for the VAE. In this way, the parameters are optimized in a mutual learning loop, and appropriate latent space for segmentation can be learned by the VAE. In experiments, we evaluated the efficiency of the proposed HVGH using real motion-capture datasets. The experimental results show that HVGH achieves more accuracy than baseline methods.

Many studies on unsupervised motion segmentation have been conducted. However, heuristic assumptions are used in

[1]Department of Mechanical Engineering and Intelligent Systems, The University of Electro-Communications, Chofu-shi, Japan
[2]Department of Systems Innovation, Osaka University, Toyonaka-shi, Japan
[3]Department of Mathematical Analysis and Statistical Inference, Institute of Statistical Mathematics, Tachikawa, Japan
[4]Department of Information Sciences, Faculty of Sciences, Ochanomizu University, Bunkyo-ku, Japan
Correspondence*: n1832072@edu.cc.uec.ac.jp

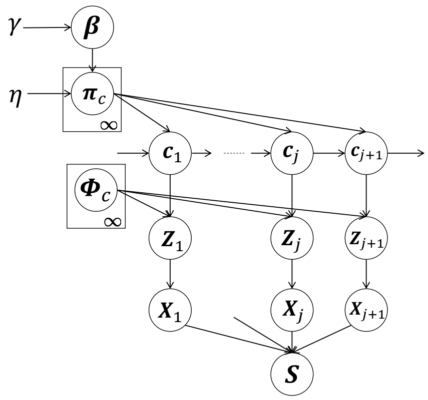

Fig. 2. Graphical model of HVGH.

many of them [5], [6], [7]. Moreover, some methods use motion features such as the zero velocity of joint angles [8], [9], [10]. However, this assumption usually leads to over-segmentation [6].

Furthermore, studies have proposed methods of detecting change points in time-series data in an unsupervised manner [11], [12], [13], [14]. These are the methods of finding points with different fluctuations based on previous observations. However, change points do not necessarily indicate the boundary of segments.

In some studies, segmentation is formulated stochastically using hidden Markov models (HMMs) [15], [16], [17], [18]. However, it is difficult for HMMs to represent complicated motion patterns. Instead, we use Gaussian processes, a type of non-parametric model that can better represent complicated time-series data compared to HMMs. We confirmed that our GP-based model can estimate segments more accurately than HMM-based methods [1].

In some studies, the number of classes is estimated by introducing a hierarchical Dirichlet process (HDP) into an HMM [15], [19]. An HDP is a method of estimating the number of classes by assuming an infinite number of classes. Fox et al. extended an HDP–HMM to make a so-called sticky HDP-HMM, which prevents over-segmentation by increasing the self-transition probability [19].

Among methods of combining probabilistic models with neural networks, a method of classifying complicated data using a GMM and VAE was proposed [20]. By contrast, our proposed HVGH is a model that combines a probabilistic model with VAE for segmenting high-dimensional time-series data.

II. Hierarchical Dirichlet Process–Variational Autoencoder–Gaussian Process–Hidden Semi-Markov Model (HVGH)

Fig. 2 shows a graphical model of our proposed HVGH, which is a generative model of time-series data. In this model, $c_j (j = 1, 2, \cdots, \infty)$ denotes the classes of the segments, where the number of classes is assumed to be countably infinite. Probability $\boldsymbol{\pi}_c$ denotes the transition probability, which is generated from the the Dirichlet process is parameterized by $\boldsymbol{\beta}$, and the $\boldsymbol{\beta}$ is generated by the GEM distribution—with the so-called stick-breaking process (SBP):

$$\boldsymbol{\beta} \sim \mathrm{GEM}(\gamma), \tag{1}$$

$$\boldsymbol{\pi}_c \sim \mathrm{DP}(\eta, \boldsymbol{\beta}). \tag{2}$$

The class c_j of the j-th segment is determined by the class of the $(j-1)$-th segment and transition probability $\boldsymbol{\pi}_c$. The segment of latent variables $\boldsymbol{Z}_j$ is generated by a Gaussian process whose parameter is $\boldsymbol{\phi}_c$, as follows:

$$c_j \sim p(c|c_{j-1}, \boldsymbol{\pi}_c, \alpha), \tag{3}$$

$$\boldsymbol{Z}_j \sim \mathcal{GP}(\boldsymbol{Z}|\boldsymbol{\phi}_{c_j}), \tag{4}$$

where $\boldsymbol{\phi}_c$ denotes a set of segments of latent variables that are classified into class c. The segment $\boldsymbol{X}_j$ is generated from the segment of the latent variables $\boldsymbol{Z}_j$ by using decoder P_{dec} of the VAE:

$$\boldsymbol{X}_j \sim p_{dec}(\boldsymbol{X}|\boldsymbol{Z}_j). \tag{5}$$

The observed sequence $\boldsymbol{s} = \boldsymbol{X}_0, \boldsymbol{X}_1, \cdots, \boldsymbol{X}_J$ is assumed to be generated by connecting segments $\boldsymbol{X}_j$ sampled by the above generative process. Similarly, the sequence of the latent variables $\bar{\boldsymbol{s}} = \boldsymbol{Z}_0, \boldsymbol{Z}_1, \cdots, \boldsymbol{Z}_J$ is obtained by connecting the segments of the latent variables $\boldsymbol{Z}_j$. In this paper, the i-th data point included in $\boldsymbol{X}_j$ is described as $\boldsymbol{x}_{ji}$, and the i-th data point included in $\boldsymbol{Z}_j$ is described as $\boldsymbol{z}_{ji}$. If the characters represent what they obviously are, we omit their subscripts.

A. Hierarchical Dirichlet Processes (HDP)

In this study, the number of segment classes is estimated by utilizing a non-parametric Bayesian model. In a non-parametric Bayesian model, an infinite number of classes is assumed, and the classes are sampled from an infinite-dimensional multinomial distribution. To realize this, an infinite-dimensional multinomial distribution must be constructed, and one of the methods for this is the SBP [3].

$$v_k \sim \mathrm{Beta}(1, \gamma) \qquad (k = 1, \cdots, \infty), \tag{6}$$

$$\beta_k = v_k \prod_{i=1}^{k-1} (1 - v_i) \qquad (k = 1, \cdots, \infty). \tag{7}$$

This process is represented as $\boldsymbol{\beta} \sim \mathrm{GEM}(\gamma)$, where "GEM" denotes the co-authors Griffiths, Engen, and McCloskey [21].

In the case of models like the HMM, all states have to share their destination states and have different probabilities of transitioning to each state. To construct such a distribution, the distribution $\boldsymbol{\beta}$ generated by the SBP is shared with all states as a base measure, and transition probabilities $\boldsymbol{\pi}_c$, which are different in each state c, are generated by another Dirichlet process. The method in which the probability distribution is constructed by a two-phase Dirichlet process is called an HDP.

$$\boldsymbol{\pi}_c \sim \mathrm{DP}(\eta, \boldsymbol{\beta}). \tag{8}$$

B. Gaussian Process (GP)

In this paper, each class represents a continuous trajectory by learning the emission z_i of time step i using a Gaussian process. In the Gaussian process, given the pairs $(\boldsymbol{i}, \boldsymbol{\phi}_c)$ of time step i and its emission, which are classified into class c, the predictive distribution of z^{new} of time step i^{new} becomes a Gaussian distribution whose parameters are μ and σ^2:

$$\begin{aligned} p(z^{new}|i^{new}, \boldsymbol{\phi}_c, \boldsymbol{i}) &\propto \mathcal{N}(z|\mu, \sigma^2), & (9)\\ \mu &= \boldsymbol{k}^T \boldsymbol{C}^{-1} \boldsymbol{i}, & (10)\\ \sigma^2 &= c - \boldsymbol{k}^T \boldsymbol{C}^{-1} \boldsymbol{k}. & (11) \end{aligned}$$

Here, $k(\cdot, \cdot)$ denotes the kernel function, and $\boldsymbol{C}$ is a matrix whose elements are

$$C(i_p, i_q) = k(i_p, i_q) + \omega^{-1}\delta_{pq}, \tag{12}$$

where ω denotes a hyperparameter that represents noise in the observations. $\boldsymbol{k}$ is a vector whose elements are $k(i_p, i^{new})$, and c is $k(i^{new}, i^{new})$. A Gaussian process can represent complicated time-series data owing to the kernel function. In this paper, we used the following kernel function, which is generally used for Gaussian processes:

$$k(i_p, i_q) = \theta_0 \exp(-\frac{1}{2}\theta_1 ||i_p - i_q||^2 + \theta_2 + \theta_3 i_p i_q), \tag{13}$$

where, θ_* denotes the parameters of the kernel.

Additionally, if the observations are composed of multi-dimensional vectors, we assume that each dimension is independently generated. Therefore, the predictive distribution $\mathcal{GP}(\boldsymbol{z}|\boldsymbol{\phi}_c)$ that the emission $\boldsymbol{z} = (z_0, z_1, \cdots)$ of time step i is generated by a Gaussian process of class c is computed as follows:

$$\begin{aligned} \mathcal{GP}(\boldsymbol{z}|\boldsymbol{\phi}_c) &= p(z_0|i, \boldsymbol{\phi}_{c,0}, \boldsymbol{i}) \\ &\quad \times p(z_1|i, \boldsymbol{\phi}_{c,1}, \boldsymbol{i}) \\ &\quad \times p(z_2|i, \boldsymbol{\phi}_{c,2}, \boldsymbol{i}) \cdots & (14)\\ &= \mathcal{N}(z|\mu_0, \sigma_0^2)\mathcal{N}(z|\mu_1, \sigma_1^2)\mathcal{N}(z|\mu_2, \sigma_2^2)\cdots. & (15) \end{aligned}$$

By using this probability, the latent variables can be classified into the classes. Moreover, because each dimension is independently generated, the mean vector $\boldsymbol{\mu}_c(i)$ and the variance-covariance matrix $\boldsymbol{\Sigma}_c(i)$ of $\mathcal{GP}(\boldsymbol{z}_{ji}|\boldsymbol{Z}_c)$ are represented as follows:

$$\begin{aligned} \boldsymbol{\mu}_c(i) &= (\mu_0, \mu_1, \mu_2, \cdots), & (16)\\ \boldsymbol{\Sigma}_c(i) &= \begin{bmatrix} \sigma_1^2 & 0 & 0 \\ 0 & \sigma_2^2 & 0 \\ 0 & 0 & \ddots \end{bmatrix}, & (17) \end{aligned}$$

where $(\mu_0, \mu_1, \mu_2, \cdots)$ and $(\sigma_0^2, \sigma_1^2, \sigma_2^2, \cdots)$ respectively represent the mean and the variance of each dimension. HVGH is a model whereby VAE and GP influence each other mutually by using $\boldsymbol{\mu}_c(i)$ and $\boldsymbol{\Sigma}_c(i)$ as the prior distribution of the VAE.

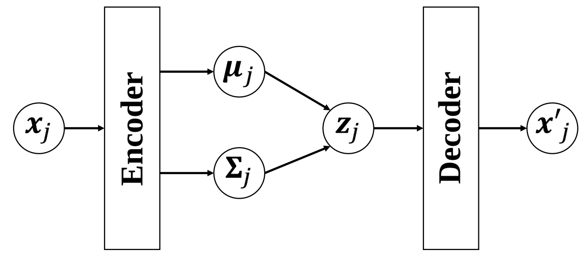

Fig. 3. Variational autoencoder (VAE).

C. Overview of the Variational Autoencoder

In this paper, we compress a high-dimensional time-series observation into low-dimensional latent variables using the VAE [4]. The VAE is a neural network that can learn the correspondence between a high-dimensional observation $\boldsymbol{x}$ and the latent variable $\boldsymbol{z}$. Fig. 3 shows an overview of the VAE. A Gaussian distribution with a mean $\boldsymbol{\mu}_{enc}(\boldsymbol{x})$ and variance $\boldsymbol{\Sigma}_{enc}(\boldsymbol{x})$ that are estimated by using encoder networks from input $\boldsymbol{x}$ is used as $q_{enc}(\boldsymbol{z})$:

$$q_{enc}(\boldsymbol{z}) = \mathcal{N}(\boldsymbol{z}|\boldsymbol{\mu}_{enc}(\boldsymbol{x}), \boldsymbol{\Sigma}_{enc}(\boldsymbol{x})). \tag{18}$$

The latent variable $\boldsymbol{z}$ is stochastically determined by this distribution, and $\boldsymbol{x}'$ is generated through decoder networks p_{dec}:

$$\begin{aligned} \boldsymbol{z} &\sim q_{enc}(\boldsymbol{z}), & (19)\\ \boldsymbol{x}' &\sim p_{dec}(\boldsymbol{x}|\boldsymbol{z}). & (20) \end{aligned}$$

The parameters of the encoder and decoder are determined to maximize the likelihood by using the variational Bayesian method. Generally, the prior distribution of the VAE is a Gaussian distribution whose mean is the zero vector $\boldsymbol{0}$, and the variance–covariance matrix is the identity matrix $\boldsymbol{e}$. On the other hand, HVGH uses a Gaussian distribution whose parameters are $\boldsymbol{\mu}_c(i)$ and $\boldsymbol{\Sigma}_c(i)$ of class c into which $\boldsymbol{z}_{ji}$ is classified. As a result, latent space suitable for segmentation can be constructed. By using this VAE, a sequence of the observation $\boldsymbol{s} = \boldsymbol{X}_0, \boldsymbol{X}_1, \cdots, \boldsymbol{X}_J$ is converted to a sequence of the latent variables $\bar{\boldsymbol{s}} = \boldsymbol{Z}_0, \boldsymbol{Z}_1, \cdots, \boldsymbol{Z}_J$ through the encoder.

III. Parameter Inference

Fig. 4 shows an outline of parameter estimation for HVGH. A sequence of observations $\boldsymbol{s}$ is converted to a sequence of latent variables $\bar{\boldsymbol{s}}$ by the VAE. Then, by the HDP-GP-HSMM, the sequence of latent variables $\bar{\boldsymbol{s}}$ is divided into segments of latent variables $\boldsymbol{Z}_0, \boldsymbol{Z}_1, \cdots$, and the parameters $\boldsymbol{\mu}_c(i)$ and $\boldsymbol{\Sigma}_c(i)$ of the predictive distribution of $\boldsymbol{z}$ are computed. This predictive distribution is used as a prior distribution of the VAE. Thus, the parameters of the VAE and HDP-GP-HSMM are mutually optimized.

A. Parameter Inference of HDP-GP-HSMM

The parameters of HDP-GP-HSMM are estimated in the same manner that we proposed in [1]. Here, we briefly explain the parameter inference and see [1] for detail.

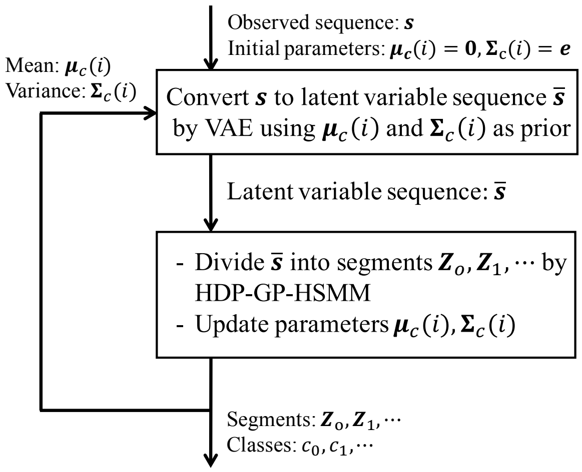

Fig. 4. Overview of parameter estimation for HVGH. The parameters are learned by a mutual learning loop of the VAE and HDP-GP-HSMM.

In the HDP-GP-HSMM, segments and classes of latent variables are determined by sampling. For efficient estimation, we utilize a blocked Gibbs sampler [22], in which all segments and their classes in one observed sequence are sampled. The segments of latent variables and their classes are sampled as follows:

$$(\boldsymbol{Z}_{n,1}, \cdots, \boldsymbol{Z}_{n,J_n}), (c_{n,1}, \cdots, c_{n,J_n}) \sim p((\boldsymbol{Z}_0, \boldsymbol{Z}_1, \cdots), (c_0, c_1, \cdots) | \bar{\boldsymbol{s}}_n). \quad (21)$$

The parameters of the Gaussian process of each class $\boldsymbol{\phi}_c$ and transition probability $p(c|c')$ are updated by using the sampled segments and their classes. However, it is difficult to compute Eq. (21) because an infinite number of classes is assumed. To overcome this problem, we use a slice sampler to compute these probabilities by stochastically truncating the number of classes.

Moreover, the probabilities of all possible patterns of segments and classifications are required in Eq. (21), and these cannot be computed naively, owing to the large computational cost. To compute Eq. (21) efficiently, we utilize forward filtering–backward sampling [23].

B. Parameter Inference of the VAE

The parameters of the encoder and decoder of VAE are estimated to maximize the likelihood $p(\boldsymbol{x})$. However, it is difficult to maximize the likelihood directly. Instead, the normal VAE maximizes the following variational lower limit:

$$\begin{aligned} L(\boldsymbol{x}_{ji}, \boldsymbol{z}_{ji}) &= \int q_{enc}(\boldsymbol{z}_{ji}|\boldsymbol{x}_{ji}) \log p_{dec}(\boldsymbol{x}_{ji}|\boldsymbol{z}_{ji}) d\boldsymbol{z}_{ji} \\ &\quad - D_{KL}(q_{enc}(\boldsymbol{z}_{ji}|\boldsymbol{x}_{ji}) || p(\boldsymbol{z}_{ji}|\mathbf{0}, \boldsymbol{e})), \end{aligned} \quad (22)$$

where $\int q_{enc}(\boldsymbol{z}_{ji}|\boldsymbol{x}_{ji}) \log p_{dec}(\boldsymbol{x}_{ji}|\boldsymbol{z}_{ji}) d\boldsymbol{z}$ represents the reconstruction error. Moreover, $p(\boldsymbol{z}_{ji}|\mathbf{0}, \boldsymbol{e})$ is a prior distribution of $\boldsymbol{z}_{ji}$, which is a Gaussian distribution whose mean is $\mathbf{0}$, and the variance–covariance matrix is $\boldsymbol{e}$.

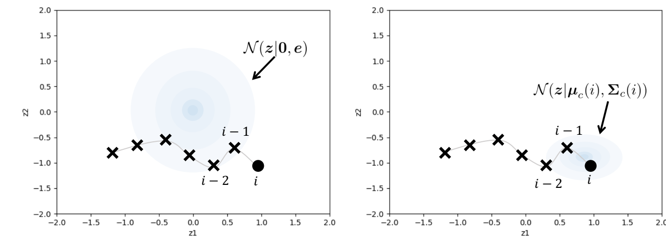

(a) (b)

Fig. 5. Influence of prior distribution. The blue region represents the standard deviation. (a) The same prior distribution is used for any data points in the normal VAE. (b) The distribution is varied depending on the time step and the class of the data point in the VAE in HVGH.

$D_{KL}(q_{enc}(\boldsymbol{z}_{ji}|\boldsymbol{x}_{ji}) || p(\boldsymbol{z}_{ji}|\mathbf{0}, \boldsymbol{e}))$ is the Kullback–Liebler divergence, and this works as a regularization term. On the other hand, in the HVGH, the mean $\boldsymbol{\mu}_c(i)$ and the variance–covariance matrix $\boldsymbol{\Sigma}_c(i)$ are used as the parameters of the prior distribution. These are the parameters of the predictive distribution of class c into which $\boldsymbol{z}_{ji}$ is classified, and they are estimated by HDP-GP-HSMM:

$$\begin{aligned} L(\boldsymbol{x}_{ji}, \boldsymbol{z}_{ji}) = \int & q_{enc}(\boldsymbol{z}_{ji}|\boldsymbol{x}_{ji}) \log p_{dec}(\boldsymbol{x}_{ji}|\boldsymbol{z}_{ji}) d\boldsymbol{z}_{ji} \\ & - D_{KL}(q_{enc}(\boldsymbol{z}_{ji}|\boldsymbol{x}_{ji}) || p(\boldsymbol{z}_{ji}|\boldsymbol{\mu}_c(i), \boldsymbol{\Sigma}_c(i))). \end{aligned} \quad (23)$$

Fig. 5 illustrates the difference in prior distribution between Eq. (22) and Eq. (23). In the normal VAE using Eq. (22), the prior distribution is $\mathcal{N}(\mathbf{0}, \boldsymbol{e})$ against all data points, as shown in Fig. 5(a). On the other hand, the parameters of the prior distribution of HVGH are computed by the Gaussian process, as shown in Fig. 5(b). Because the GP restricts data points that have closer time steps to being more similar values, z_{ji} becomes a similar value to $z_{j,i-1}$ and $z_{j,i+1}$. Therefore, the latent space learned by the VAE can reflect the characteristics of time-series data. Moreover, these parameters have different values depending on the class of the data point. Therefore, the latent space can also reflect the characteristics of each class.

IV. Experiments

To validate the proposed HVGH, we applied it to several types of time-series data. For comparison, we used HDP-GP-HSMM [1], HDP-HMM [15], HDP-HMM+NPYLM [16], BP-HMM [17], and Autoplait [18] as baseline methods.

A. Datasets

To evaluate the validity of the proposed method, we used the following four motion-capture datasets.

- **Chicken dance:** We used a sequence of motion capture data of a human performing a chicken dance from the CMU Graphics Lab Motion Capture Database[1]. The dance includes four motions, as shown in Fig. 6.

[1] `http://mocap.cs.cmu.edu/`: subject 18, trial 15

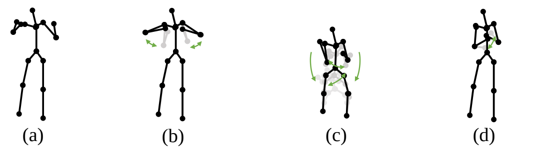

Fig. 6. Four unit motions included in the chicken dance: (a) beaks, (b) wings, (c) tail feathers, and (d) claps.

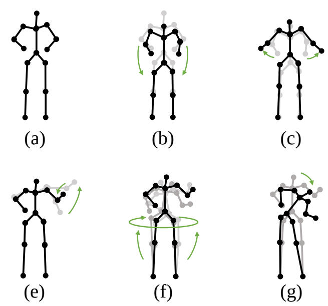

Fig. 7. Seven unit motions included in the "I'm a little teapot" dance: (a) short and stout, (b) bending knee, (c) spread arms, (d) handle, (e) spout, (f) steam up, and (g) pour.

- **"I'm a little teapot" dance (teapot dance):** We also used two sequences from the teapot dance motion-capture data from subject 29 in the CMU Graphics Lab Motion Capture Database[2]. These sequences include seven motions, as shown in Fig. 7.
- **Exercise motion 1:** To determine the validity against more complicated motions, we used three sequences of exercise motion-capture data from subject 13 in the CMU Graphics Lab Motion Capture Database. These sequences include seven motions, as shown in Fig. 8.
- **Exercise motion 2:** Further, we used three sequences of different exercises from the motion-capture data from subject 14 in the CMU Graphics Lab Motion Capture Database. These sequences include 11 motions, as shown in Fig. 9.

To reduce computational cost, all the sequences were preprocessed by down sampling to 4 fps. These motion-capture datasets included the directions of 31 body parts, each of which was represented by a three-dimensional Euler angle. Therefore, each frame was constructed in 93-dimensional vectors. We used sequences of 93-dimensional vectors as input. Moreover, HVGH requires hyperparameters, and we set them to $\lambda = 14.0, \theta_0 = 1.0, \theta_1 = 1.0, \theta_2 = 0.0, \theta_3 = 16.0$, which were determined empirically for segmentation of the 4-fps sequences. For the chicken dance exclusively, we set λ to half that of the others, because its motion-capture data was shorter than the others. To train the VAE, we used $1/4$ of all the data points as a mini batch, Adam [24] was used for optimization, and optimization was iterated 150 times. To train HDP-GP-HSMM, the blocked Gibbs sampler was iterated 10 times to converge the parameters. Furthermore, the mutual learning loop of the VAE and HDP-GP-HSMM was iterated until the variational lower limit converged.

[2]`http://mocap.cs.cmu.edu/`: subject 29, trials 3 and 8

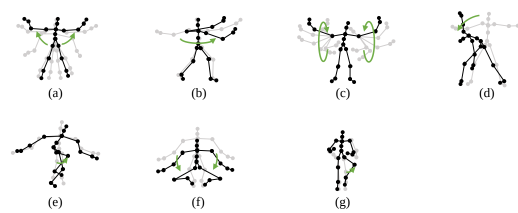

Fig. 8. Seven unit motions included in exercise motion 1: (a) jumping jack, (b) twist, (c) arm circle, (d) bend over, (e) knee raise, (f) squatting, and (g) jogging

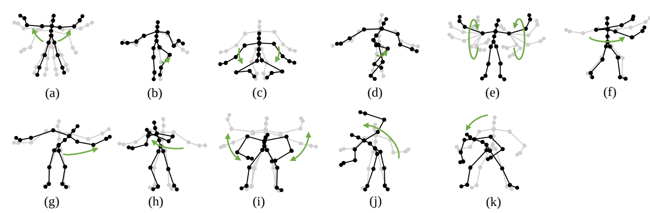

Fig. 9. Eleven unit motions included in exercise motion 2: (a) jumping jack, (b) jogging, (c) squatting, (d) knee raise, (e) arm circle, (f) twist, (g) side reach, (h) boxing, (i) arm wave, (j) side bend, and (k) toe touch.

B. Segmentation of Motion-capture Data

To evaluate the segmentation accuracy, we used four measures: the normalized Hamming distance, precision, recall, and F-measure as with [1]. An estimated boundary point is treated as correct if the estimated boundary is within $\pm 5\%$ of the sequence length.

First, we applied baseline methods to the 93-dimensional time-series data. However, the baseline methods were not able to segment the 93-dimensional time-series data appropriately because of high dimensionality. Therefore, we applied the VAE with the same parameters as HVGH, and sequences of three-dimensional latent variables were used for segmentation of the baseline methods. Tables I, II, III, and IV show the results of segmentation on each of the four motion-capture datasets.

VAE+HDP-GP-HSMM and VAE+BP-HMM were able to segment the motion-capture data from the chicken dance and teapot dance. However, in the results with exercise motion by VAE+BP-HMM, the value of the normalized Hamming distance was larger and the F-measure was smaller than those of the dance motions. This is because simple and discriminative motions were repeated in the chicken dance and the teapot dance. Therefore, BP-HMM, which is an HMM-based model, was able to segment them. By contrast, the Gaussian process used in HVGH and HDP-GP-HSMM is non-parametric, making it possible to represent complicated motion patterns in the exercise data. Moreover, HVGH achieved more accurate segmentation than HDP-GP-HSMM. We believe that this is because the appropriate latent space for the segmentation was constructed by using the predictive distribution of the GP as the prior distribution of the VAE in HVGH.

TABLE I

SEGMENTATION RESULTS FOR THE CHICKEN DANCE.

	Hamming distance	Precision	Recall	F-measure	# of estimated classes
HVGH	0.23	0.86	0.86	0.86	4
VAE+HDP-GP-HSMM	0.31	1.0	0.71	0.83	4
VAE+HDP-HMM	0.74	0.15	1.0	0.26	11
VAE+ HDP-HMM+NPYLM	0.48	1.0	0.86	0.92	7
VAE+BP-HMM	0.34	1.0	0.86	0.92	3
VAE+Autoplait	0.66	0.0	0.0	0.0	1

TABLE II

SEGMENTATION RESULTS FOR THE TEA POTS DANCE.

	Hamming distance	Precision	Recall	F-measure	# of estimated classes
HVGH	0.28	0.71	0.83	0.77	7
VAE+HDP-GP-HSMM	0.26	1.0	0.64	0.78	6
VAE+HDP-HMM	0.73	0.01	1.0	0.17	17
VAE+ HDP-HMM+NPYLM	0.41	0.72	0.93	0.81	9
VAE+BP-HMM	0.28	0.50	0.86	0.63	10
VAE+Autoplait	0.75	0.0	0.0	0.0	1

TABLE III

SEGMENTATION RESULTS FOR THE EXERCISE MOTION: SUBJECT 13.

	Hamming distance	Precision	Recall	F-measure	# of estimated classes
HVGH	0.16	0.66	0.93	0.75	11
VAE+HDP-GP-HSMM	0.24	0.53	0.93	0.67	12
VAE+HDP-HMM	0.75	0.05	1.0	0.09	10
VAE+ HDP-HMM+NPYLM	0.61	0.30	1.0	0.45	28
VAE+BP-HMM	0.58	0.29	0.97	0.44	7
VAE+Autoplait	0.76	0.0	0.0	0.0	2

TABLE IV

SEGMENTATION RESULTS FOR THE EXERCISE MOTION: SUBJECT 14.

	Hamming distance	Precision	Recall	F-measure	# of estimated classes
HVGH	0.20	0.50	1.0	0.66	13
VAE+HDP-GP-HSMM	0.29	0.45	1.0	0.62	12
VAE+HDP-HMM	0.78	0.04	1.0	0.07	24
VAE+ HDP-HMM+NPYLM	0.69	0.22	1.0	0.36	26
VAE+BP-HMM	0.79	0.48	0.81	0.55	5
VAE+Autoplait	0.79	0.0	0.0	0.0	3

Furthermore, the number of motion classes in the chicken dance and teapot dance was correctly estimated by HVGH. In the exercise motion, the larger numbers were estimated because their sequences included complicated motions. In the case of exercise motion 1, 11 classes were estimated by HVGH—more than the correct number seven. This is because that the stationary state was estimated as a unit of motion, and symmetrical motion was separately classified as left-sided and right-sided motion in different classes. Moreover, 13 classes—more than the correct number 11—were estimated by HVGH in exercise motion 2. Again, this is because stationary motion was estimated as one motion, and because the symmetrical motion shown in Fig. 9(j) was divided into two classes: left- and right-sided motion. However, it is reasonable to estimate the stationary state as a unit of motion. Further, dividing a symmetrical motion into two classes was not erroneous, because the observed values for the left- and right-sided motion were different. Therefore, we conclude that HVGH yielded better results in this case.

With regard to exercise motion 1, Fig. 10 shows the latent

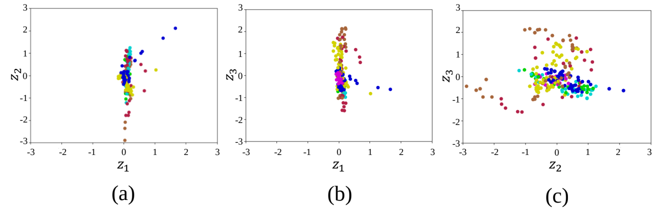

Fig. 10. Latent space of the VAE.

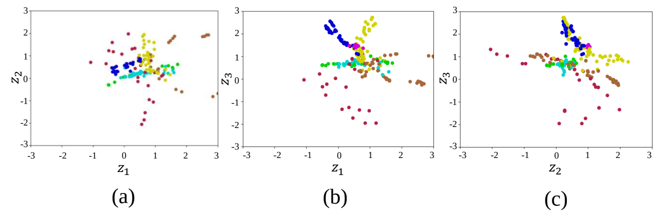

Fig. 11. Latent space of the HVGH.

variables estimated by the VAE, and Fig. 11 shows the latent variables learned by mutual learning with HVGH. In these figures, (a), (b), and (c) respectively represent the first and second, first and third, and second and third dimension of the latent variables. The color of each point reflects the correct motion class. In Fig. 10, latent variables do not necessarily reflect the motion class because they were estimated with the VAE exclusively. By contrast, in Fig. 11, the latent variables in the same class have more similar values. This means that a latent space is estimated representing the features of unit motions.

From these results, we conclude that HVGH can estimate the correct number of classes and accurate segments from high-dimensional data by using the proposed mutual learning loop.

V. CONCLUSION

In this paper, we proposed HVGH, which segments high-dimensional time-series data by mutual learning of a VAE and HDP-GP-HSMM. In the proposed method, high-dimensional vectors are converted to low-dimensional latent variables representing features of unit motions with the VAE. Using these latent variables, HVGH achieves accurate segmentation. The experimental results showed that the segments, their classes, and the number of classes could be estimated correctly using the proposed method. Moreover, the results showed that HVGH is effective with various types of high-dimensional time-series data compared to a model where the VAE and HDP-GP-HSMM are used independently.

However, the computational cost of HVGH is very high, because it takes $O(N^3)$ to learn N data points using a Gaussian process, and this is repeated in the mutual learning loop. Because of this problem, HVGH cannot be applied to large-scale time-series data. We plan to reduce the computational cost by introducing the approximation method for the Gaussian process proposed in [25], [26].

Moreover, in order to simplify the computation, we assumed that the dimensions of the observation were independent, and we consider this assumption reasonable because the experimental results showed that the proposed method works well. However, the dimensions of the observation are not actually independent, and the dependency between the dimensions will need to be considered in order to model more complicated whole-body motion. We believe that multi-output Gaussian processes can be used to represent dependencies between dimensions [27], [28].

Acknowledgments

This work was supported by JST CREST Grant Number JPMJCR15E3 and JSPS KAKENHI Grant Number JP18H03295.

References

[1] M. Nagano, T. Nakamura, T. Nagai, D. Mochihashi, I. Kobayashi, and M. Kaneko, "Sequence Pattern Extraction by Segmenting Time Series Data Using GP-HSMM with Hierarchical Dirichlet Process," International Conference on Intelligent Robots and Systems, pp. 4067–4074, 2018.

[2] Y. W. Teh, M. I. Jordan, M. J. Beal, and D. M. Blei, "Hierarchical Dirichlet processes," Journal of the American Statistical Association, vol. 101, no. 476, pp. 1566–1581, 2006.

[3] J. V. Gael, Y. Saatci, Y. W. Teh, and Z. Ghahremani, "Beam Sampling for the Infinite Hidden Markov Model," International Conference on Machine Learning, pp. 1088–1095, 2008.

[4] D. P. Kingma and M, Welling, "Auto-Encoding Variational Bayes," arXiv preprint arXiv:1312.6114, 2014.

[5] M. Wächter and T. Asfour, "Hierarchical segmentation of manipulation actions based on object relations and motion characteristics," International Conference on Advanced Robotics (ICAR), pp. 549–556, 2015.

[6] R. Lioutikov, G. Neumann, G. Maeda, and J. Peters, "Probabilistic segmentation applied to an assembly task," IEEE-RAS International Conference on Humanoid Robots, pp. 533–540, 2015.

[7] W. Takano and Y. Nakamura, "Real-time unsupervised segmentation of human whole-body motion and its application to humanoid robot acquisition of motion symbols," Robotics and Autonomous Systems, vol. 75, pp. 260–272, 2016.

[8] A. Fod, M.J. Matarić, and O.C. Jenkins, "Automated derivation of primitives for movement classification," Autonomous Robots, vol. 12, no. 1, pp. 39–54, 2002.

[9] T. Shiratori, A. Nakazawa, and K. Ikeuchi, "Detecting dance motion structure through music analysis," IEEE International Conference on Automatic Face and Gesture Recognition, pp. 857–862, 2004.

[10] J.F.S. Lin and D. Kulić, "Segmenting human motion for automated rehabilitation exercise analysis," Conference of IEEE Engineering in Medicine and Biology Society, pp. 2881–2884, 2012.

[11] D. Haber, A.A.C. Thomik, and A.A. Faisal, "Unsupervised Time Series Segmentation for High-Dimensional Body Sensor Network Data Streams," International Conference on Wearable and Implantable Body Sensor Networks, pp. 121–126, 2014.

[12] S. Liu, M. Yamada, N. Collier, and M. Sugiyama, "Change-Point Detection in Time-Series Data by Relative Density-Ratio Estimation," arXiv preprint arXiv:1203.0453v2, 2013.

[13] R. Lund, X.L. Wang, Q.Q. Lu, J. Reeves, C. Gallagher, and Y. Feng, "Changepoint Detection in Periodic and Autocorrelated Time Series," American Meteorological Society, vol. 20, no. 20, pp. 5178–5190, 2007.

[14] Y. Kenji and T. Jun-ichi, "A Unifying Framework for Detecting Outliers and Change Points from Non-stationary Time Series Data," Proceedings of the Eighth ACM SIGKDD International Conference on Knowledge Discovery and Data Mining, vol. 18, pp. 676–681, 2002.

[15] M.J. Beal,, Z. Ghahramani, and C.E. Rasmussen, "The infinite hidden Markov model," In Advances in Neural Information Processing Systems, pp. 577–584, 2001.

[16] T. Taniguchi and S. Nagasaka, "Double articulation analyzer for unsegmented human motion using Pitman–Yor language model and infinite hidden Markov model, " In IEEE/SICE International Symposium on System Integration, pp. 250–255, 2011.

[17] E.B. Fox, E.B. Sudderth, M.I. Jordan, and A.S. Willsky, "Joint modeling of multiple related time series via the beta process," arXiv preprint arXiv:1111.4226, 2011.

[18] Y. Matsubara, Y. Sakurai, and C. Faloutsos, "Autoplait: Automatic mining of co-evolving time sequences," ACM SIGMOD International Conference on Management of Data, pp. 193–204, 2014.

[19] E.B. Fox, E.B. Sudderth, M.I. Jordan, and A.S. Willsky, "The sticky HDP-HMM: Bayesian nonparametric hidden Markov models with persistent states", Annals of Applied Statistics, vol. 5, no. 2A, pp. 1020–1056, 2011

[20] M.J. Johnson, D. Duvenaud, A.B. Wiltschko, S.R. Datta, R.P. Adams, "Composing graphical models with neural networks for structured representations and fast inference," arXiv preprint arXiv:1603.06277v5, 2017.

[21] J. Pitman, "Poisson-Dirichlet and GEM invariant distributions for splitand-merge transformations of an interval partition," Combinatorics, Probability and Computing, vol. 11, pp. 501–514, 2002.

[22] C.S. Jensen, U. Kjærulff, and A. Kong, "Blocking Gibbs sampling in very large probabilistic expert systems," International Journal of Human-Computer Studies, vol. 42, no. 6, pp. 647–666, 1995.

[23] K. Uchiumi, T. Hiroshi, and D. Mochihashi, "Inducing Word and Part-of-Speech with Pitman-Yor Hidden Semi-Markov Models," Joint Conference of the 53rd Annual Meeting of the Association for Computational Linguistics and the 7th International Joint Conference on Natural Language Processing, pp.1774–1782, 2015.

[24] Diederik P. Kingma, and Jimmy Lei Ba, "ADAM: A METHOD FOR STOCHASTIC OPTIMIZATION," arXiv:1412.6980v9, 2017.

[25] D. Nguyen-Tuong, J.R. Peters, and M. Seeger, "Local Gaussian process regression for real time online model learning and control," In Advances in Neural Information Processing Systems, pp. 1193–1200, 2009.

[26] Y. Okadome, K. Urai, Y. Nakamura, T. Yomo, and H. Ishiguro, "Adaptive lsh based on the particle swarm method with the attractor selection model for fast approximation of Gaussian process regression," Artificial Life and Robotics, vol. 19, pp.220–226, 2014.

[27] M. Álvarez, D. Luengo, M. Titsias, and N. Lawrence, "Efficient multioutput Gaussian processes through variational inducing kernels," Proceedings of the Thirteenth International Conference on Artificial Intelligence and Statistics, pp. 25–32, 2010.

[28] R. Dürichen, M.A.F. Pimentel, L. Clifton, A. Schweikard, and D.A. Clifton, "Multitask Gaussian processes for multivariate physiological time-series analysis," IEEE Transactions on Biomedical Engineering, vol. 62, no. 1, pp. 314–322, 2015.